Journal of Power Sources 196 (2011) 3773–3780

Contents lists available at ScienceDirect

Journal of Power Sources

journal homepage: www.elsevier.com/locate/jpowsour

Optimization of polytetrafluoroethylene content in cathode gas diffusion layer by the evaluation of compression effect on the performance of a proton exchange membrane fuel cell

Hao-Ming Chang[a], Chien-Wei Lin[a], Min-Hsing Chang[a,*], Huan-Ruei Shiu[b], Wen-Chen Chang[b], Fang-Hei Tsau[b]

[a] Department of Mechanical Engineering, Tatung University, 40, 3rd Sec., Chun-Shan North Rd., Taipei 104, Taiwan
[b] New Energy Technology Division, Energy and Environment Research Laboratories, Industrial Technology Research Institute/ITRI, Hsinchu 310, Taiwan

ARTICLE INFO

Article history:
Received 28 November 2010
Received in revised form
17 December 2010
Accepted 17 December 2010
Available online 8 January 2011

Keywords:
Proton exchanger membrane fuel cell
Gas diffusion layer
Microporous layer
Polytetrafluoroethylene
Compression ratio

ABSTRACT

This research investigates the optimal polytetrafluoroethylene (PTFE) content in the cathode gas diffusion layer (GDL) by evaluating the effect of compression on the performance of a proton exchange membrane (PEM) fuel cell. A special test fixture is designed to control the compression ratio, and thus the effect of compression on cell performance can be measured in situ. GDLs with and without a microporous layer (MPL) coating are considered. Electrochemical impedance spectroscopy (EIS) is used to diagnose the variations in ohmic resistance, charge transfer resistance and mass transport resistance with compression ratio. The results show that the optimal PTFE content, at which the maximum peak power density occurs, is about 5 wt% with a compression ratio of 30% for a GDL without an MPL coating. For a GDL with an MPL coating, the optimal PTFE content in the MPL is found to be 30% at a compression ratio of 30%.

1. Introduction

The gas diffusion layer (GDL) is a key component that may significantly affect the performance of a proton exchange membrane (PEM) fuel cell. In particular, the amount of hydrophobic agents such as polytetrafluoroethylene (PTFE) in the GDL is an important factor that dominates the GDL's water transport properties and also the water balance within the membrane–electrode assembly (MEA). An appropriate PTFE content in the GDL, especially on the cathode side, not only prevents flooding of the electrode under high-humidity conditions but also avoids drying of the MEA under low-humidity conditions. Numerous studies have been devoted to determining the optimal hydrophobic agent content in the cathode GDL with or without a microporous layer (MPL) coating on one side of the GDL's surface [1–13]. However, all of them either neglect the influence of compression in theoretical analyses or describe experiments performed under constant assembly pressure conditions. For example, Yan et al. [5] used fluorinated ethylene propylene (FEP) as the hydrophobic agent and found that the best cell performance can be achieved with an FEP content of 10% in the GDL and 20% in the MPL. However, the compression ratio or assembly pressure used in their experiments is unclear.

The compression ratio of the GDL induced by assembly pressure is also an important factor that may profoundly affect cell performance. Insufficient compression may cause serious gas leakage and a large contact resistance, which lead to poor performance and potentially dangerous operating conditions. In contrast, overcompression may change the GDL's pore structure and hence increase the mass transfer resistance through the GDL, which also degrades cell performance. Therefore, it is critical to determine the optimal compression ratio during fuel cell assembly. Numerous studies in the literature have investigated this question [14–31]. However, most of them did not consider the effect of the PTFE content of the GDL. Only a few investigations have used different types of GDL [14,15] and explored their characteristics under different compression ratios. Since both the assembly pressure and PTFE content may change the pore structures and affect the transport resistance of reactants through the GDL and MPL, it is necessary to take the effect of compression into consideration in the determination of the optimal PTFE content in the gas diffusion media. So far it is still unclear how compression affects the determination of the optimal PTFE content within the GDL and MPL, and this fact motivates the present investigation.

* Corresponding author. Tel.: +886 2 25925252x3410; fax: +886 2 25997142.
E-mail address: mhchang@ttu.edu.tw (M.-H. Chang).

0378-7753/$ – see front matter © 2011 Elsevier B.V. All rights reserved.
doi:10.1016/j.jpowsour.2010.12.090

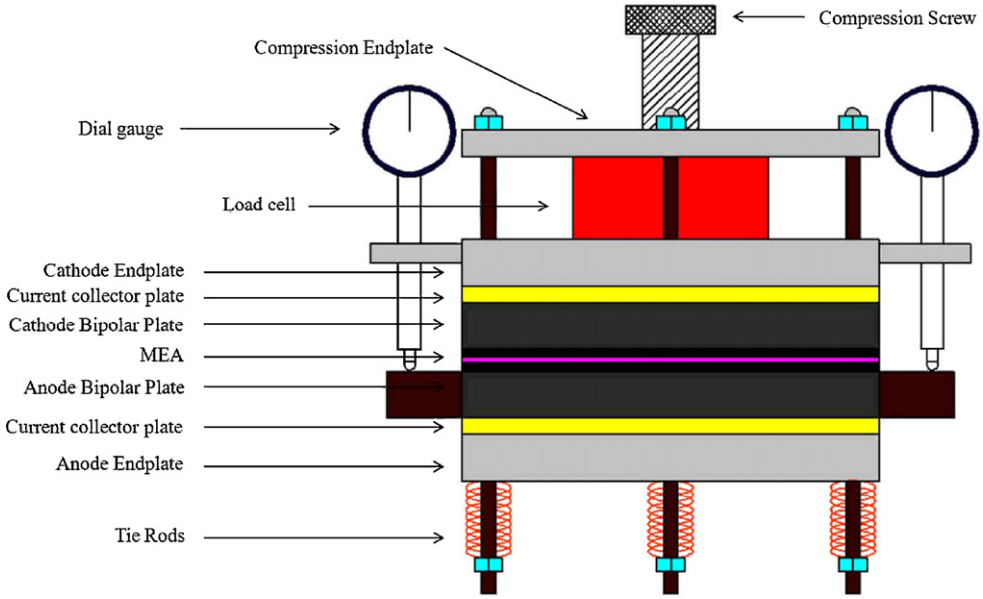

Fig. 1. Fuel cell test fixture design.

In this study, we design and construct a special test fixture to investigate the effect of compression on the performance of a PEM fuel cell. The present design can adjust the compression ratio in situ, so cell performance can be measured directly after the compression ratio on the cell is adjusted. Electrochemical impedance spectroscopy (EIS) is also used to diagnose the variations in ohmic resistance, charge transfer resistance, and mass transport resistance with compression. Cathode GDLs both with and without an MPL coating are considered in order to determine the optimal PTFE content in the GDL and MPL. The results clarify the effect of compression on the determination of the optimal PTFE content of the cathode GDL and MPL.

2. Experimental

2.1. Single cell fixture design

Fig. 1 shows a schematic of the special single fuel cell test fixture; photographs of the top and side views are shown in Fig. 2(a) and (b), respectively. The fixture consists of an MEA, two graphite flow field plates, two current collectors, and two end plates. The anode end plate rests against two stainless steel prisms fastened to the base of a stainless steel plate. Thus, it is fixed during the compression process, whereas the cathode end plate is movable. A central compression screw is used to exert a compression force on the fuel cell unit. The magnitude of the compression force is measured by a load cell installed between the compression screw and the cathode end plate. To achieve uniform compression, eight bolts evenly distributed on the boundary are used to align the compression after the central screw is rotated until the readings on both dial gauges are the same. The dial gauges not only indicate the uniformity of the compression but also provide the readings for determining the compression ratio. Two electrical heaters are buried in each end plate to provide heating during the test procedures. This special fixture makes it possible to adjust the compression ratio while the fuel cell remains in operation.

2.2. MEA preparation and experimental materials

The MEA consists of a catalyst-coated proton exchange membrane (CCM) and two GDLs on opposite sides of the CCM. In this study, all the experiments employ the same CCM, which is made of Nan-Ya®, series number bMEA5. The GDLs are attached to either side of the CCM directly to form the MEA. The reaction area on the CCM is 5 cm × 5 cm. Since we are interested in the optimisation of PTFE content in the cathode GDL, the anode GDL is controlled to be the same in all tests. SGL® carbon paper 10BA without an

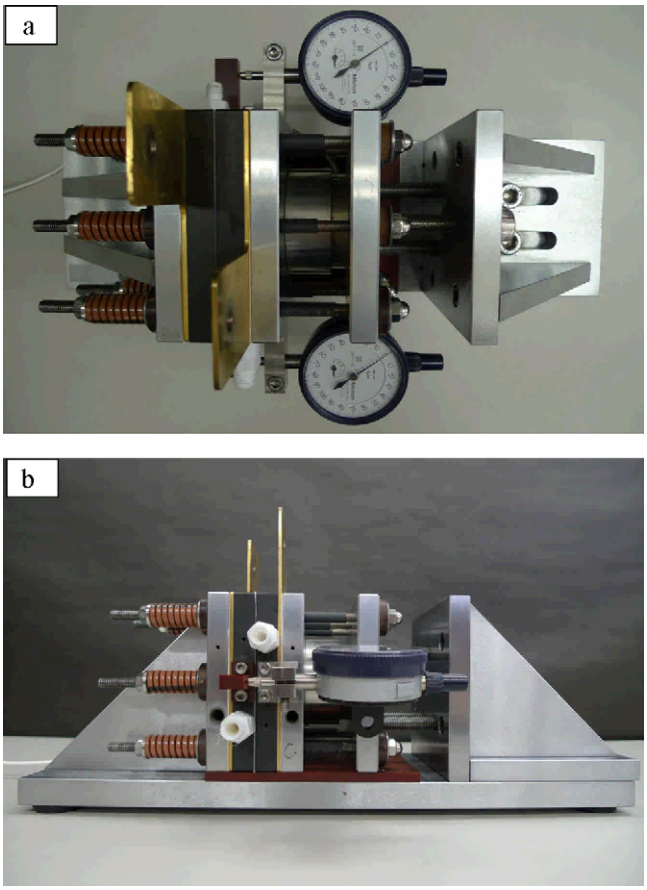

Fig. 2. Photographs of (a) top and (b) side views of the fuel cell fixture.

MPL coating is used as the anode GDL. Cathode GDLs with different PTFE contents are made from SGL® 10AA carbon paper without any wet-proofing treatment. To adjust the PTFE content in the cathode carbon paper, the paper is first washed with acetone to remove possible surface contaminants. Then it is dipped in diluted PTFE solution to incorporate PTFE into it. Next, it is placed in a mechanical convection oven to dry at 110 °C and 250 °C for 20 min each. These processes are repeated several times until the desired PTFE content has been reached. Finally, the carbon paper is placed in a high-temperature oven for sintering at 350 °C. To prepare GDLs with an MPL coating, a carbon slurry is prepared from a mixture of carbon powder (Vulcan XC72R carbon black) and ethylene glycol with a pre-assigned weight percentage of PTFE. The mixture is sonicated in an ultrasonic cleaner and then agitated by a dispersing instrument for 2 h to ensure sufficient mixing of the carbon powder and PTFE. Next, the carbon slurry is sprayed uniformly on the surface of the carbon paper to form an MPL and then dried in a convection oven at 90 °C. This spraying and drying process is repeated several times until the carbon loading reaches 1.0 mg cm^{-2}. Finally, the carbon paper is sintered in a high-temperature oven at 350 °C to complete the MPL coating.

The flow field plate is made of Poco graphite material AXF-5QC with two parallel serpentine channels machined on one side of its surface. The current collectors are made of copper with a pure gold coating on their surfaces. Gaskets made of soft polymer material were used around the border of the MEA to prevent leakage of the reaction gases. The overall thickness of the gasket is slightly less than that of the MEA. Therefore, the MEA is compressed first, and then the MEA together with the gasket can be compressed uniformly. The compression ratio is defined as the variation in MEA thickness over its original thickness. That is,

$$\text{Compression ratio} = \frac{\Delta l}{l_m + l_a + l_b} \times 100\%, \quad (1)$$

where l_m, l_a, and l_b are the original thicknesses of the CCM, anode GDL, and cathode GDL, respectively. The variation in thickness Δl is read from the dial gauges on the test fixture.

2.3. Performance tests and characteristic analysis

The experimental measurements focus on the effect of compression on cell performance with respect to different PTFE contents in the cathode GDL and MPL. Therefore, cell performance was measured under several different compression ratios. A Hephas® P-300 fuel cell test station was employed to measure the cell performance and obtain the polarization curves. Pure hydrogen and compressed air were used as the fuel and the oxidant, respectively. The flow rates of hydrogen and air were controlled by mass flow controllers (MFCs) with maximum flow rates of 2000 sccm and 5000 sccm, respectively. Both reactant gases were humidified by bubbling the gases through distilled water tanks held at a constant temperature of 70 °C. The temperature of the cell was also held at 70 °C in all experiments. Before measuring the polarization curve, the MEA was conditioned for at least 24 h to ensure that the cell performance is stablized. During the testing processes, the flow rates of hydrogen and air were first held at minimum values of 200 sccm and 500 sccm, respectively, and then they were adjusted automatically to stoichiometric values of 1.5 and 2.0 for hydrogen and air, respectively. The polarization curves were obtained by scanning the cell potential from an open circuit voltage (OCV) to 0.3 V and then recording the resulting current densities. In each case the scanning process repeated three times and the recorded current densities were averaged to determine the polarization curve. The maximum error in current densities at the same cell potential is found to be less than 5%. Each test always began at a compression ratio of 10%, and then the compression ratio was increased gradually to a maximum of 35%.

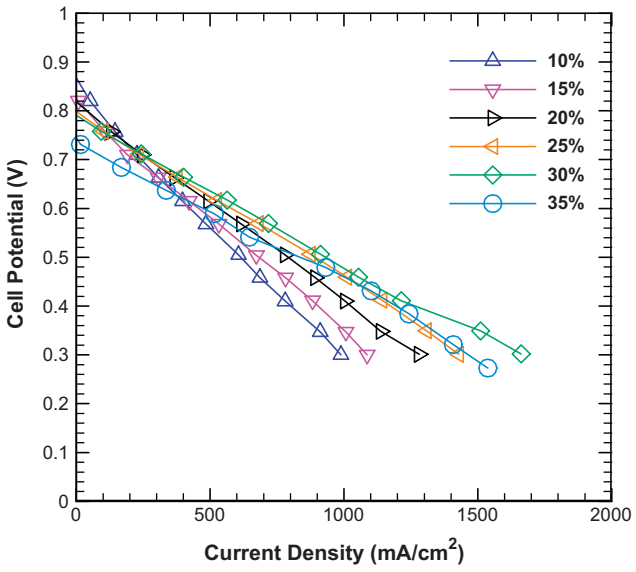

Fig. 3. Polarization curves at different compression ratios. PTFE content is 5% in cathode carbon paper without an MPL coating.

To identify the individual contributions to the cell resistance, a frequency response analyzer (FRA) module added to an Autolab PGSTAT 302N potentiostat was employed to perform the EIS measurements. The impedance spectra were recorded by sweeping frequencies over the range of 10 μHz to 1 MHz with the amplitude of the AC current held at 5% of that of the DC current. The sweeping process also repeated at least three times to assure the same spectrum was reproducible. The obtained spectra were further analyzed by an equivalent circuit to explore the effects of compression on the variations in ohmic resistance, charge transfer resistance, and gas transfer resistance. In addition to the polarization curve and impedance spectra measurements, the physical properties of the GDLs were also measured, including gas permeability and in-plane electrical resistivity. The gas permeability was measured by a PMI® gas permeability tester using air as the test gas. The measured air flow rate and applied pressure difference were converted to the permeability according to Darcy's law. To measure the in-plane electrical resistivity, a low-resistivity meter (Loresta-GP®, model MCP-T610) based on the four-point test method was used in compliance with the JIS-K-7194 standard. The obtained data increase our understanding of the effect of PTFE content on the performance of the GDL and MPL.

3. Results and discussion

The tests can be divided into two parts. First, we consider cathode GDLs without an MPL coating. The optimal PTFE content is determined by evaluating the variations in the OCV, peak power density, and limiting current density under different compression ratios. Second, the influence of the MPL is considered, and carbon paper is coated with MPLs of varying PTFE contents to determine the optimal PTFE content.

3.1. Cathode GDLs without MPL coating

The polarization curves of a typical case with a 5% PTFE content in the cathode GDL are shown in Fig. 3 for several compression ratios. Obviously, the cell performance depends heavily on the compression acting on it. For a compression ratio of 10%, the

cell is apparently under insufficient compression, since the cell potential descends rapidly with increasing current density. Insufficient compression could cause high electrical contact resistances within the cell, resulting in poor cell performance due to high ohmic resistance. As the compression ratio increases, cell performance improves; the limiting current density measured at 0.3 V increases up to a compression ratio of 30% and then decreases at a compression ratio of 35%. However, the OCV appears to decrease significantly with increasing compression ratio. The OCV is well known to be quite sensitive to fuel crossover and/or internal current within the cell [32]. A small change in fuel crossover may cause a very noticeable voltage drop at an open circuit. Accordingly, the present results indicate that a larger compression ratio will enhance the amount of fuel crossover and thus reduce the cell potential at an open circuit. Similar results can also be observed in other cases with different PTFE contents in the cathode carbon paper.

To determine the optimal PTFE content in the cathode GDL, the variations in OCV, peak power density, and limiting current density with compression ratio for four typical cases with different PTFE contents are demonstrated in Fig. 4(a)–(c), respectively. As shown in Fig. 4(a), the maximum value of the OCV in each case is about 0.86 V and always occurs at a compression ratio of 10%. This value is lower than that of a typical PEM fuel cell, which is generally higher than 0.9 V. The main reason is the lack of an MPL coating on the surface of the carbon paper facing the CCM. The morphology of the carbon paper surface is quite rough without this coating. Roughness at the interface between the CCM and the carbon paper may enhance the amount of fuel crossover and cause a significant drop in the OCV. This effect is more pronounced when the cell is under a higher compression ratio. Thus, the OCV decreases with increasing compression ratio in all cases. In particular, at moderate compression (20–30%), a higher PTFE content in the GDL seems to degrade the cell potential at an open circuit. In Fig. 4(b), the variation in peak power density with PTFE content is limited when the compression is insufficient, as indicated in the case with a 10% compression ratio. As the compression ratio increases, the influence of the PTFE content grows, indicating that it is an important factor dominating the cell performance. Although the peak power density rises gradually in all cases, the rate of increase is larger in the GDLs with lower PTFE contents. At compression ratios of 25% and 30%, in particular, the peak power density appears to decrease with increasing PTFE content, and the maximum occurs at a PTFE content of 5%. Similar behaviour can also be observed in the variation in limiting current density, as shown in Fig. 4(c). Since a PTFE content of 5% yields the maximum peak power density and limiting current density at an appropriate compression ratio of 30%, we suggested that it is the optimal PTFE content in the cathode carbon paper.

To better understand the effects of compression and PTFE content on the fuel cell, AC impedance spectroscopy was used to diagnose cell performance. Impedance spectra at a current density of 800 mA cm^{-2} as a function of compression ratio are shown in Fig. 5 for a PTFE content of 5% in the cathode carbon paper. Two distinct arcs can be observed, which have been widely reported in the literature for a hydrogen/air PEM fuel cell operating on fully humidified reactants. Similar spectra also appear in the other cases with different PTFE contents. The high-frequency arc on the left represents mainly the effective charge transfer resistance for the oxygen reduction reaction in the catalyst layer, and the low-frequency arc on the right is attributed mainly to the transport resistance of air within the GDL. The generally proposed equivalent circuit shown in Fig. 5 was used to simulate the impedance data. The horizontal real axis intercept of the impedance spectrum at the end of the left arc is equal to the ohmic resistance of the fuel cell R_1. The resistance R_2 and capacitance C_1 represent the effective charge transfer

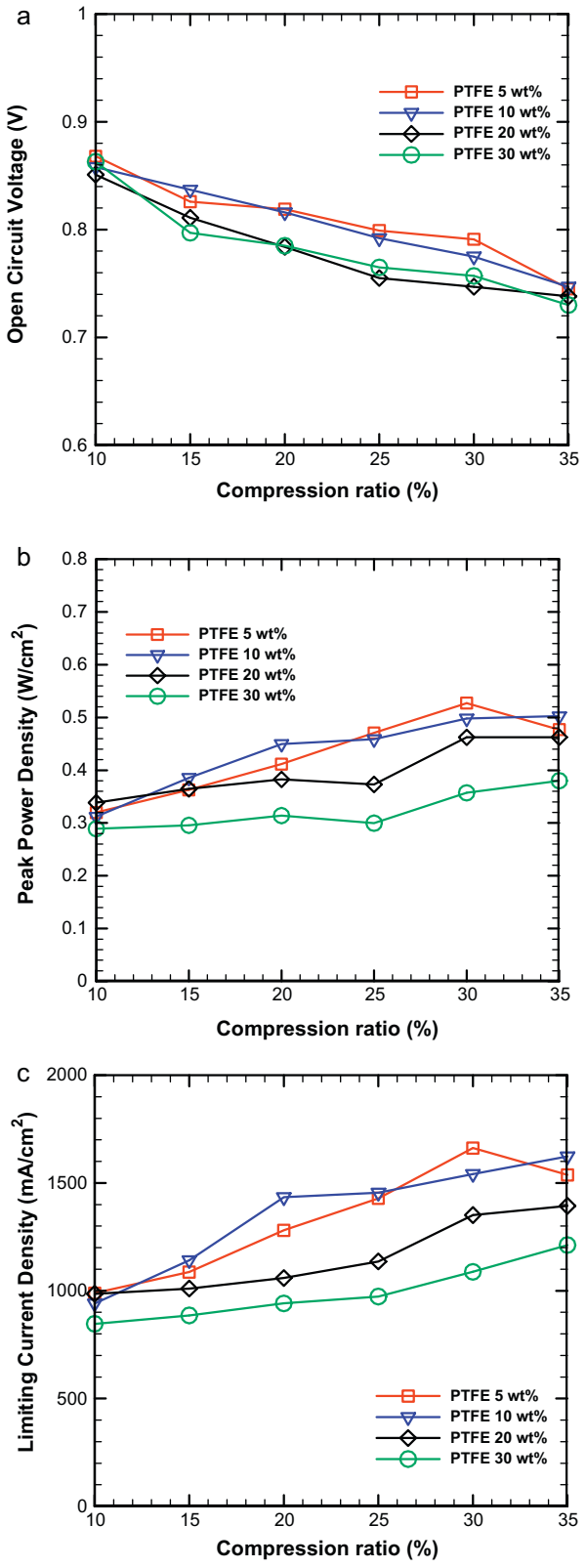

Fig. 4. Variations in (a) OCV, (b) peak power density, and (c) limiting current density with compression ratio in cathode GDLs with different PTFE contents.

resistance and the associated capacitance properties of the catalyst layer, respectively. The resistance R_3 represents the transfer resistance of air, and C_2 is the associated capacitance. As demonstrated in Fig. 5, the resistance R_1 decreases and shifts significantly to the left with increasing compression ratio up to a compres-

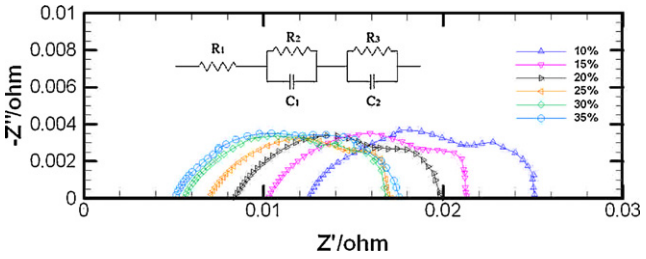

Fig. 5. Impedance spectra at different compression ratios with a current density of 800 mA cm^{-2}. PTFE content is 5% in cathode carbon paper without an MPL coating.

sion ratio of 30%. The reduction in R_1 with a further increase to 35% is relatively insignificant. This result indicates that the compression will be adequate at a compression ratio of 30%, and the electrical contact resistance at the interfaces between the fuel cell components could be minimized at this compression ratio. Thus, the ohmic resistance R_1 can represent the membrane resistance appropriately once the fuel cell has reached sufficient compression. The variations in ohmic resistance R_1, charge transfer resistance R_2, and gas transfer resistance R_3 with compression ratio are displayed in Fig. 6(a)–(c), respectively, for four typical cases with different PTFE contents in the cathode GDL. As shown in Fig. 6(a), the ohmic resistance decreases gradually with the compression ratio in all cases. However, for a given compression ratio, the variation in R_1 is relatively limited at PTFE contents of 5–20%, especially when the compression ratio is greater than 20%. Moreover, in these cases the compression seems to be adequate at a compression ratio of 30%. However, when the PTFE content rises to 30%, an obvious increase in R_1 appears, and the contribution from the electrical contact resistance is still significant even when the compression ratio reaches 35%. In Fig. 6(b), in all the cases the charge transfer resistance R_2 decreases gradually with increasing compression ratio, indicating that sufficient compression efficiently enhances the fuel cell reaction kinetics. Under insufficient compression (a compression ratio of less than 25%), we did not find any regular behaviour for the variation in R_2 with compression ratio. However, under sufficient compression (at compression ratios 25% and 30%), the resistance R_2 first increases with increasing PTFE content up to 20% and then jumps to a lower value at a PTFE content of 30% under the same compression ratio. The variations are relatively limited at a compression ratio of 35%. Fig. 6(c) suggests that both the compression ratio and the PTFE content of the GDL profoundly affect the gas transfer resistance R_3. This resistance is due mainly to the diffusion of hydrogen and air to the anode and cathode catalyst layers, respectively, through the GDL. As shown in Fig. 6(c), R_3 always increases with increasing compression ratio. This trend indicates that an increase in compression always results in a higher gas transport resistance, since the pores for the passage of reaction gas within the GDL will be condensed, blocking the diffusion of gas through the GDL. The saturation of liquid water within the pores of the cathode GDL may also increase under higher compression, increasing the air transport resistance. Moreover, at the same compression ratio, the gas transfer resistance always increases with increasing PTFE content in the cathode GDL. Note also that the increasing rate is slower at a PTFE content of 5%, at which the gas transfer resistance appears to be minimized under normal compression. Table 1 lists the permeabilities and in-plane electrical resistances measured before compression for the four typical cases with different PTFE contents. The permeability decreases gradually with increasing PTFE content, whereas the in-plane electrical resistance rises slightly at first until the PTFE content reaches 20% and then has a more significant increase at a 30% PTFE content.

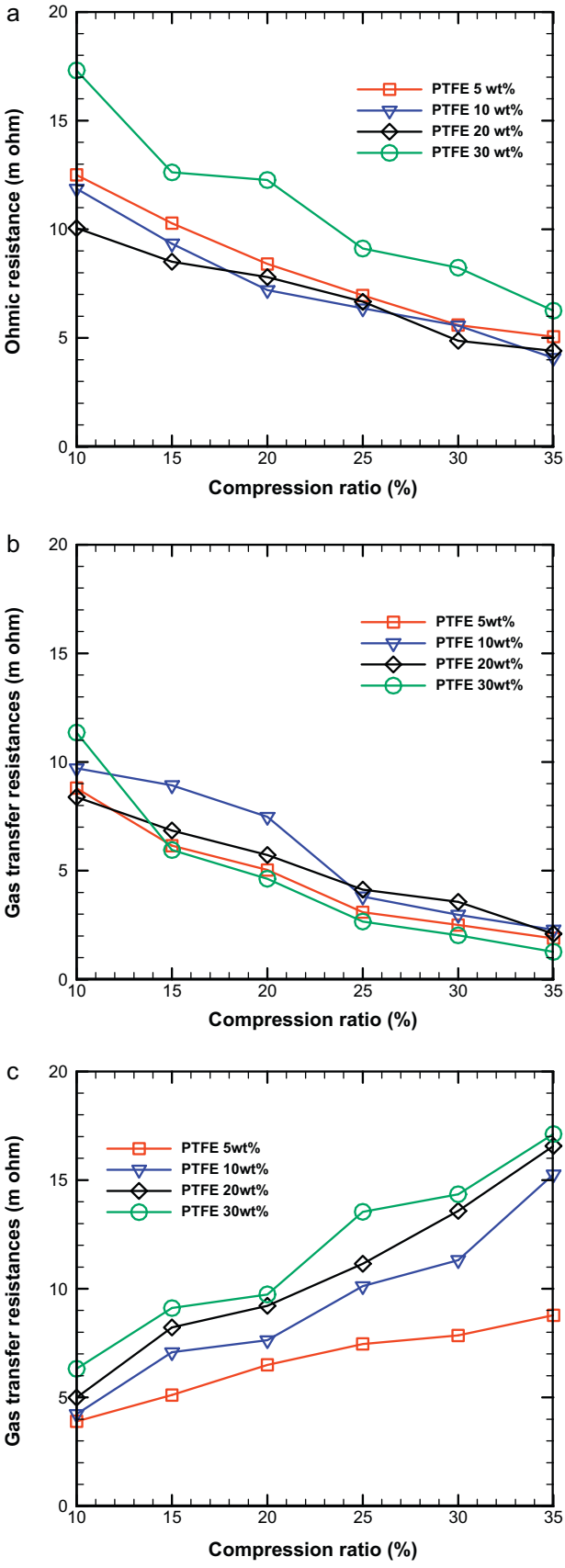

Fig. 6. Variations in (a) ohmic resistance, (b) charge transfer resistance, and (c) gas transfer resistance with compression ratio at different PTFE contents in the cathode GDL.

Table 1
Permeabilities and in-plane electrical resistances at different PTFE contents in GDL without MPL coating.

PTFE content (%)	Permeability (m^2)	In-plane electrical resistance (mΩ cm)
5	2.76×10^{-11}	42.16
10	2.43×10^{-11}	43.58
20	2.33×10^{-11}	44.28
30	2.16×10^{-11}	57.48

3.2. Cathode GDLs with an MPL coating

Since we have found that carbon paper with a 5% PTFE content gives the best performance under normal compression, here we further consider the influence of the MPL coating in this case and try to find the optimal PTFE content in the MPL. The polarization curves of a typical case with a 5% PTFE content in the MPL are shown in Fig. 7 at different compression ratios. A comparison with the results of Fig. 3 clearly shows that the addition of an MPL on the cathode carbon paper can effectively enhance fuel cell performance. The limiting current density measured at 0.3 V increases gradually with the compression ratio and exhibits no degradation even at a compression ratio of 35%. Note that it is quite difficult to check whether the limiting current density will begin to reverse at higher compression ratios by increasing the compression ratio further using the test fixture shown in Fig. 2. However, over-compression can still be observed by examining the variation in OCV with compression ratio. As shown in Fig. 7, the OCV now rises to more than 0.9 V after the employment of an MPL on the cathode carbon paper, suggesting that the MPL coating may effectively reduce the amount of fuel crossover. The only exception is that at a compression ratio of 35%, the OCV is still less than 0.9 V. This result reveals that the effect of fuel crossover is more significant in this case and indicates that the fuel cell is over-compressed at a compression ratio of 35%. The variations in the polarization curves for the other cases with different PTFE contents in the MPL were also obtained. To determine the optimal PTFE content in the MPL, here we follow the method used in Section 3.1 to separately consider the variations in OCV, peak power density, and limiting current density with compression ratio at different PTFE contents in the MPL. The results are presented in Fig. 8(a)–(c), respectively. As shown in Fig. 8(a), the

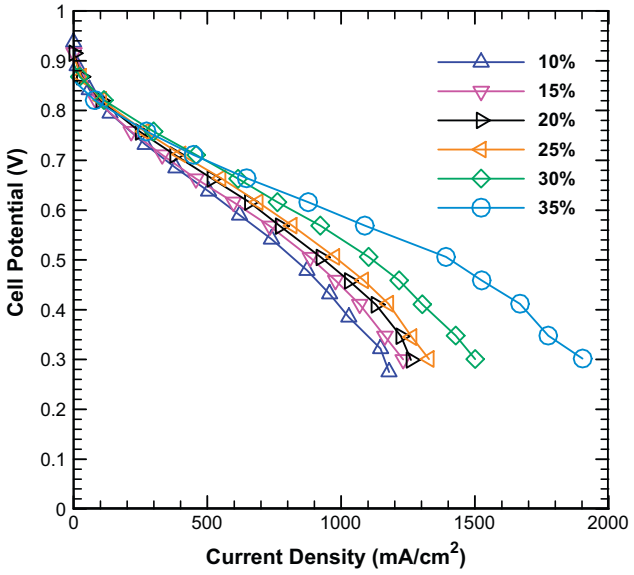

Fig. 7. Polarization curves at different compression ratios for cathode carbon paper with an MPL coating. PTFE content of the cathode MPL is 5%.

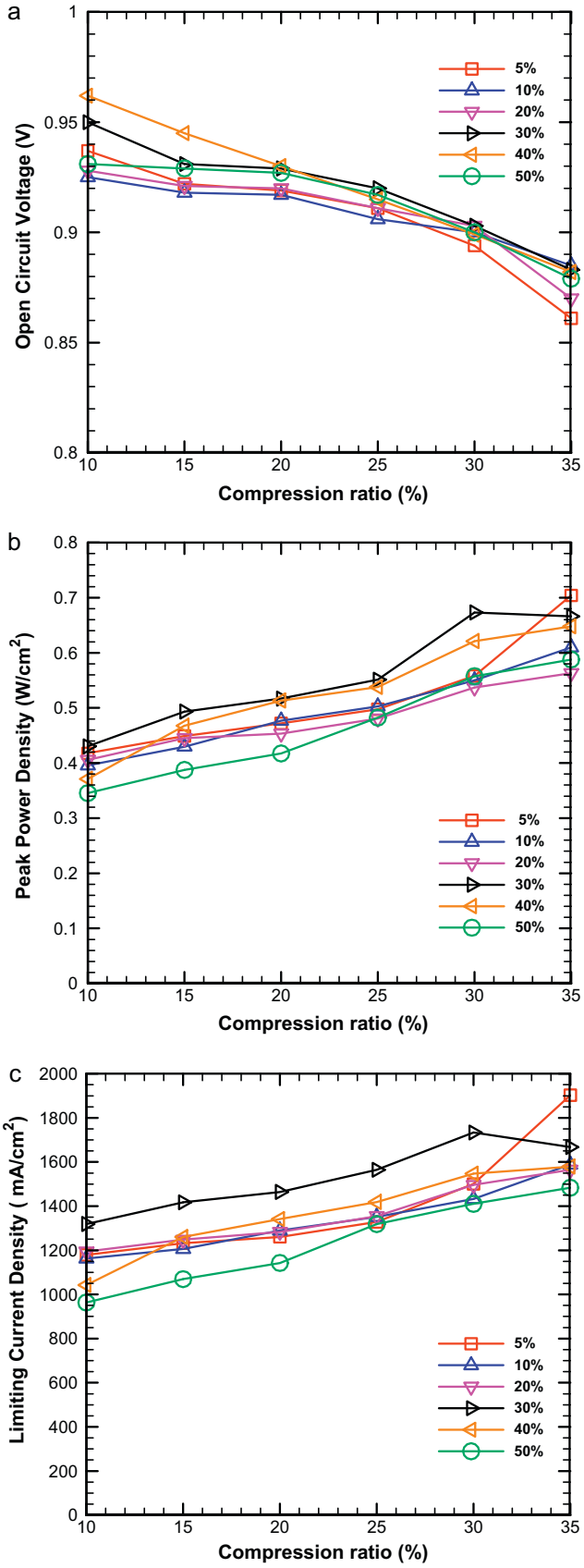

Fig. 8. Variations in (a) OCV, (b) peak power density, and (c) limiting current density with compression ratio at different PTFE contents in the cathode MPL.

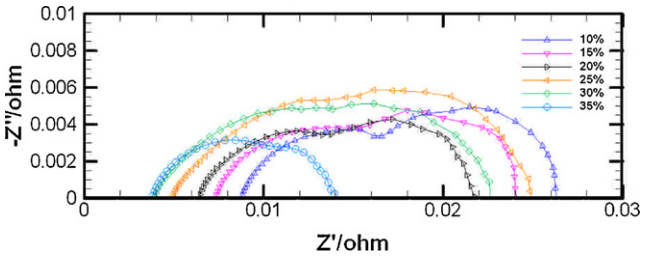

Fig. 9. Impedance spectra at different compression ratios with a current density of 800 mA cm^{-2}. PTFE content of the cathode MPL is 5%.

OCV in each case generally decreases slowly up to a compression ratio of 30% and then jumps to a significantly lower value at a compression ratio of 35%. Moreover, the OCV in each case is generally greater than 0.9 V at compression ratios of less then 30% and less than 0.9 V at a compression ratio of 35%. That is, over-compression can always be observed at a compression ratio of 35%. Fig. 8(b) shows that the peak power density in each case rises monotonically with compression ratio except at 30% PTFE content, in which case the peak power density is less at a compression ratio of 35% than at 30%. Furthermore, at a compression ratio of 30%, a 30% PTFE content also yields the maximum peak power density before over-compression occurs. The variations in limiting current density are similar to those in peak power density, as shown in Fig. 8(c). In particular, a PTFE content of 30% always yields the highest limiting current density at compression ratios of 30% or lower. Since this case exhibits the highest peak power density and limiting current density at a proper compression ratio of 30%, and the corresponding OCV remains above 0.9 V, we may conclude that the optimal PTFE content in the MPL is 30%.

AC impedance spectra as a function of compression ratio are shown in Fig. 9 for a typical case with a 5% PTFE content in the MPL at a current density of 800 mA cm^{-2}. Each spectrum contains two distinct arcs similar to those shown in Fig. 5. Therefore, the same equivalent circuit can be used to simulate the variations in ohmic resistance, charge transfer resistance, and gas transfer resistance. We first note that the ohmic resistance, represented by the left intercept on the horizontal real axis, shifts gradually to the left with increasing compression up to a compression ratio of 30% and then stops decreasing at a compression ratio of 35%. This result is consistent with that for the case without an MPL coating shown in Fig. 5, which indicates that a 30% compression ratio is necessary to eliminate the electrical contact resistance even with an MPL coating on the carbon paper. The variations in ohmic resistance with compression ratio at different PTFE contents in the MPL are shown in Fig. 10(a). The ohmic resistance is generally considered to be due mainly to proton transport through the membrane, and thus the measured ohmic resistance indicates the membrane resistance. However, the present results show that the PTFE content in the MPL may also affect the ohmic resistance somewhat under sufficient compression. The associated variations in the charge and gas transfer resistances are shown in Fig. 10(b) and (c), respectively. The effects of compression on both resistances are similar to those illustrated in Fig. 6(b) and (c) for the case without an MPL coating. That is, higher compression may improve the reaction kinetics and thus reduce the charge transfer resistance. Simultaneously, the gas transfer resistance increases gradually with compression, increasing more quickly once the compression ratio exceeds 25%, as shown in Fig. 10(c). In particular, a PTFE content of 30% always yields the lowest ohmic and gas transfer resistances, making this the optimal PTFE content in the MPL. Table 2 lists the measured permeabilities and in-plane electrical resistances for the six cases at different PTFE contents in the MPL. A comparison with Table 1 clearly shows that the permeability decreases after the MPL coating is added to

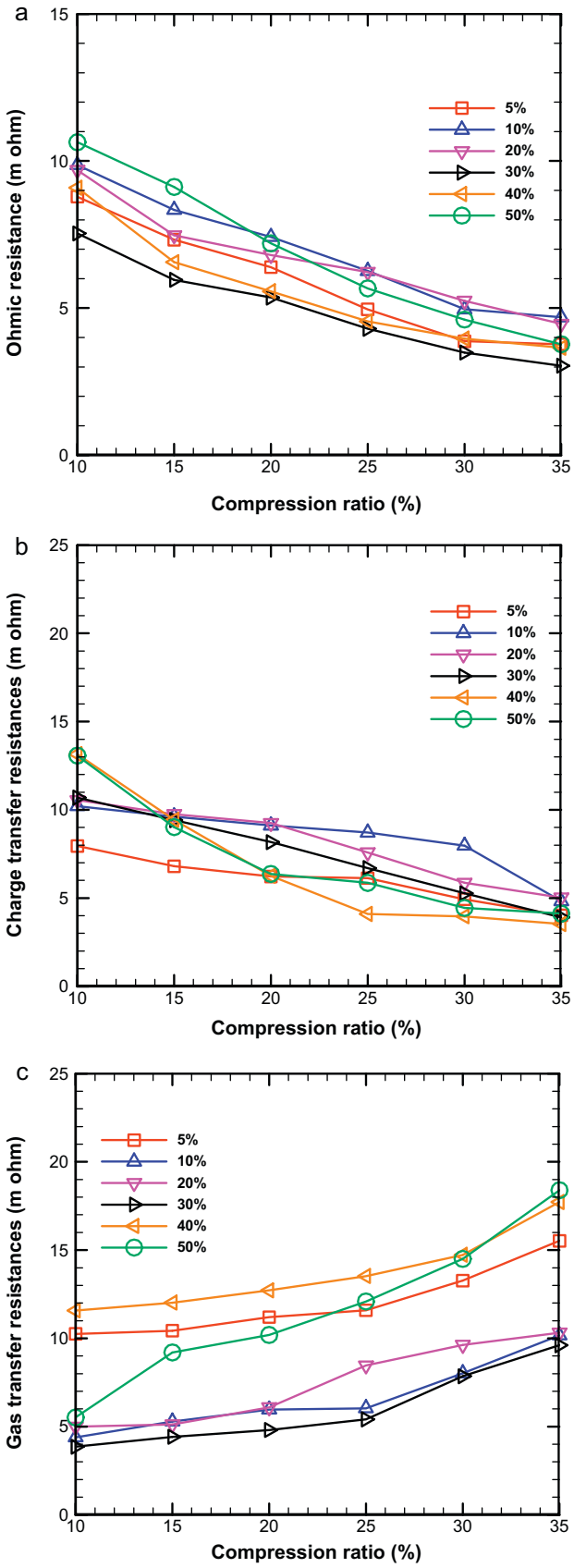

Fig. 10. Variations in (a) ohmic resistance, (b) charge transfer resistance, and (c) gas transfer resistance with compression ratio at different PTFE contents in the cathode MPL.

Table 2
Permeabilities and in-plane electrical resistances at different PTFE contents in MPL.

PTFE content in MPL (%)	Permeability (m^2)	In-plane electrical resistance (mΩ cm)
5	9.55×10^{-12}	35.74
10	8.78×10^{-12}	41.38
20	8.34×10^{-12}	43.64
30	7.77×10^{-12}	44.39
40	6.91×10^{-12}	46.93
50	6.27×10^{-12}	50.80

the GDL's surface. The permeability also decreases gradually with increasing PTFE content in the MPL, and the in-plane electrical resistance appears to rise slightly. Although the maximum permeability and minimum in-plane electrical resistance do not occur at a PTFE content of 30% in the MPL, this PTFE content still provides the best cell performance. Since the function of the MPL is to improve the transport of liquid water and avoid flooding within the cathode GDL, the present results indicate that the cell performance depends more heavily on the PTFE content in the MPL than on the permeability or in-plane electrical resistance. A PTFE content of 30% seems to provide better water transport ability than the others and should be the optimal PTFE content in the MPL.

4. Conclusions

In this study, a special fuel cell test fixture was designed and used to measure the effect of compression on fuel cell performance in situ. The purpose was to evaluate the optimal PTFE content of both the GDL and the MPL by measuring the fuel cell performance at different compression ratios. The results show that appropriate compression and proper PTFE content in both the GDL and the MPL are quite important in determining the optimal fuel cell performance. For a GDL without an MPL coating, a GDL containing 5% PTFE yielded the maximum power density at a compression ratio of 30%. This case also shows less OCV loss due to fuel crossover and a minimum gas transfer resistance at sufficient compression. Therefore, we suggest that it is the optimal PTFE content in the cathode GDL. Furthermore, in a GDL with an MPL coating, we found that the optimal PTFE content in the MPL is 30%, since the fuel cell exhibits the best performance at this PTFE content under the same compression ratio of 30%. The present fuel cell test fixture design provides an efficient way of measuring fuel cell performance under different compression ratios. Its use could be expanded in the future to evaluate the effect of compression on the determination of the optimal design parameters in a PEM fuel cell system.

Acknowledgments

The authors gratefully acknowledge the financial support from Industrial Technology Research Institute (ITRI) and National Science Council of Taiwan through the Grant NSC 95-2623-7-132-001.

References

[1] G.G. Park, Y.J. Sohn, T.H. Yang, Y.G. Yoon, W.Y. Lee, C.S. Kim, J. Power Sources 131 (2004) 182–187.
[2] C. Lim, C.Y. Wang, Electrochim. Acta 49 (2004) 4149–4156.
[3] P.M. Wilde, M. Mandle, M. Murata, N. Berg, Fuel Cell 4 (2004) 180–184.
[4] G. Lin, T.V. Nguyen, J. Electrochem. Soc. 152 (2005) A1942–A1948.
[5] W.M. Yan, C.Y. Hsueh, C.Y. Soong, F. Chen, C.H. Cheng, S.C. Mei, Int. J. Hydrogen Energy 32 (2007) 4452–4458.
[6] G. Velayutham, J. Kaushik, N. Rajalakshmi, K.S. Dhathathreyan, Fuel Cell 7 (2007) 314–318.
[7] J.H. Lin, W.H. Chen, Y.J. Su, T.H. Ko, Energy Fuel 22 (2008) 1200–1203.
[8] S. Park, J.W. Lee, B.N. Popov, J. Power Sources 177 (2008) 457–463.
[9] J.H. Tian, Z.Y. Shi, J.S. Shi, Z.Q. Shan, Energy Convers. Manage. 49 (2008) 1500–1505.
[10] W. Dai, H. Wang, X.Z. Yuan, J. Martin, J. Shen, M. Pan, Z. Luo, J. Power Sources 188 (2009) 122–126.
[11] W.M. Yan, D.K. Wu, X.D. Wang, A.L. Ong, D.J. Lee, A. Su, J. Power Sources 195 (2010) 5731–5734.
[12] T. Kitahara, T. Konomi, H. Nakajima, J. Power Sources 195 (2010) 2202–2211.
[13] M.S. Ismail, T. Damjanovic, K. Hughes, D.B. Ingham, L. Ma, M. Pourkashanian, M. Rosli, J. Fuel Cell Sci. Technol. 7 (2010) 051016.
[14] W.K. Lee, C.H. Ho, J.W.V. Zee, M. Murthy, J. Power Sources 84 (1999) 45–51.
[15] J.H. Lin, W.H. Chen, Y.J. Su, T.H. Ko, Fuel 87 (2008) 2420–2424.
[16] S.J. Lee, C.D. Hsu, C.H. Huang, J. Power Sources 145 (2005) 353–361.
[17] J. Ge, A. Higier, H. Liu, J. Power Sources 159 (2006) 922–927.
[18] A. Bazylak, D. Sinton, Z.S. Liu, N. Djilali, J. Power Sources 163 (2007) 784–792.
[19] I. Nitta, T. Hottinen, O. Himanen, M. Mikkola, J. Power Sources 171 (2007) 26–36.
[20] P. Zhou, C.W. Wu, G.J. Ma, J. Power Sources 163 (2007) 874–881.
[21] P. Zhou, C.W. Wu, J. Power Sources 170 (2007) 93–100.
[22] T. Hottinen, O. Himanen, S. Karvonen, I. Nitta, J. Power Sources 171 (2007) 113–121.
[23] T. Hottinen, O. Himanen, Electrochem. Commun. 9 (2007) 1047–1052.
[24] Y. Zhou, G. Lin, A.J. Shih, S.J. Hu, J. Power Sources 163 (2007) 777–783.
[25] Z.Y. Su, C.T. Liu, H.P. Chang, C.H. Li, K.J. Huang, P.C. Sui, J. Power Sources 183 (2008) 182–192.
[26] I. Nitta, S. Karvonen, O. Himanen, M. Mikkola, Fuel Cell 8 (2008) 410–421.
[27] Y. Zhou, G. Lin, A.J. Shih, S.J. Hu, J. Power Sources 192 (2009) 544–551.
[28] Y. Zhou, G. Lin, A.J. Shih, S.J. Hu, ASME J. Fuel Cell Sci. Technol. 6 (2009) 041005.
[29] Z. Shi, X. Wang, L. Guessous, ASME J. Fuel Cell Sci. Technol. 7 (2010) 021012.
[30] X.Q. Xing, K.W. Lum, H.J. Poh, Y.L. Wu, J. Power Sources 195 (2010) 62–68.
[31] Y.H. Lai, Y. Li, J.A. Rock, J. Power Sources 195 (2010) 3215–3223.
[32] J. Larminie, A. Dicks, Fuel Cell Systems Explained, John Wiley & Sons Ltd., England, 2003.